

Model of Mobile Manipulator Performance Measurement using SysML

Roger Bostelman^{1,2}  · Sebti Fofou^{2,3} · Tsai Hong¹ · Mili Shah⁴

Received: 5 April 2017 / Accepted: 17 September 2017
© US Government (outside the USA) 2017

Abstract Test methods for measuring safety and performance of mobile manipulators have yet to be developed. Therefore, potential mobile manipulator users cannot compare one system to another. Systems Modeling Language (SysML) is a general-purpose modeling language for systems engineering applications that supports the specification, analysis, design, verification, and validation of simple through complex systems, such as mobile manipulators. As test methods are developed to allow performance comparison of the varied mobile manipulators, so to should be the case of allowing comparison of most any mobile manipulator configuration and control strategy during performance measurements. Additionally, mobile manipulator manufacturers and users can then compare these systems to tasks using various methods. This paper uses SysML to describe two measurement methods (optical tracking and artifacts) and the performance measurement of mobile manipulators performing assembly tasks. The SysML models are verified through systems review, referenced experimentation and summarize with uncertainty propagation models of the mobile manipulator.

Keywords Systems modeling language (SysML) · Mobile manipulator · Performance measurement · Standards · Test methods · Control

1 Introduction

Robot arms mounted on mobile bases or “mobile manipulators”¹ offer high mobility and manipulability. However, test methods for measuring the functionality, safety, and performance of these mobile manipulators have yet to be developed. As a result, potential users of mobile manipulator are unable to compare one system to another. A key component of creating test methods is that a given mobile manipulator must align with expected parameters such as reach, speed, dexterity, and manipulability. In addition, mobile manipulator control must be easy to understand so that users can rapidly and effectively program the system to perform as expected. Model Based Systems Engineering (MBSE) provides a simplified representation to model a given mobile manipulator system. Specifically, Systems Modeling Language (SysML) is a graphical modeling language that supports the “specification, analysis, design, verification, and validation of systems that include hardware, software, data, personnel, procedures and facilities” [1].

SysML provides four essential tools or pillars: Structure (with definition and use), Behavior (with interaction state machines, and activity/function), Requirements, and Parametrics (with equations and units). Very large projects

✉ Roger Bostelman
roger.bostelman@nist.gov

¹ National Institute of Standards and Technology, Gaithersburg, MD 20899, USA

² Le2i, Université de Bourgogne, BP 47870, 21078 Dijon, France

³ Computer Science, New York University Abu Dhabi, P.O. Box 129188, Abu Dhabi, UAE

⁴ Loyola University Maryland, 4501 N. Charles Street, Baltimore, MD 21210, USA

¹Commercial equipment, software, and materials are identified in order to adequately specify certain procedures. In no case does such identification imply recommendation or endorsement by the National Institute of Standards and Technology, nor does it imply that the materials, equipment, or software are necessarily the best available for the purpose.

with multi-user access may suggest a different modeling language, such as Teamcenter System Engineering (TCSE) [2]. However, modeling the performance measurement of mobile manipulators is ideally suited for SysML as Rahman, et al. make a similar case for using SysML in the design of mobile robots [3]. In this work, the software for a mobile robot is developed using MBSE with SysML since the creation of reusable software modules for programming the robot results in platform independent design and a reduction in development time. While this work demonstrates that SysML can be applied to some robotic systems with varying degrees of success, the authors do not describe how it might be applicable to other robot application domains. Additionally, Rahman, et al suggest that SysML is uniquely suited for accurately modeling increasingly complex and physical robotics systems, as well as for creating a standard approach useful across many different industries. They state “Instead of modeling the hardware or software of the system, we are instead considering a generalized system in a given domain, and modeling the capabilities of the generalized system for the application domain. This helps illustrate the flexibility of SysML in being able to model a wide variety of robotic systems from a number of different perspectives.”

The objective of this paper is to apply SysML modeling to the performance measurement of mobile manipulators. Specifically, this paper uses SysML to describe two measurement methods and the performance measurement of mobile manipulators performing assembly tasks. The paper expands upon the research in [4], of mobile manipulator performance measurement using a novel artifact, to also include the use of an optical tracking measurement system. For example, more detailed information is described through models: the interconnected mobile manipulator system and subsystems, methods of performance measurement (search and bisect) and overall sequential timing of the performance measurement experiments and potential real world implementation. Previous experiments have occurred and verify the mobile manipulator performance measurement concepts modeled in this paper where some reiteration from these references are provided for the reader’s convenience. The SysML models are verified through review of the systems being used in this iteration, including the mobile base (AGV), manipulator (robot arm), and measurement systems. The models are also verified through referenced experimentation and summarized with uncertainty propagation models of the mobile manipulator. Although it may also be possible, through software code development modules provided in some SysML compilers, to provide actuation and sensing capability for complex systems such as mobile manipulators, the intent of this paper was to provide a simple, generic model of the various systems..

This paper is organized as follows. Section 2 describes the relative complexity of the mobile manipulator and its interconnections, where an example mobile manipulator system was used to develop and verify the SysML system models. Section 3 describes the performance measurement systems used to measure the mobile manipulator, including a novel artifact-based system and an optical tracking system. Section 4 verifies the developed SysML models while Section 5 describes the uncertainty propagation that demonstrates a theoretical basis inherent in performance measurement of any mobile manipulator. Section 6 describes a use case for the performance measurement of mobile manipulators as modeled using SysML for both the artifact and optical tracking measurement systems. Finally, Section 7 concludes the paper.

2 Mobile Manipulator System

An example of a mobile manipulator system that was used as basis for this paper is shown in Fig. 1. The system is used for developing mobile manipulator performance test methods and for uncertainty measurements under the National Institute of Standards and Technology (NIST) Robotic Systems for Smart Manufacturing Program [5]. This program provides “the measurement science needed to enable all manufacturers, including small and medium ones, to characterize and understand the performance of robotics systems within their enterprises.” The mobile manipulator shown in Fig. 1 provides a collaborative robot measurement

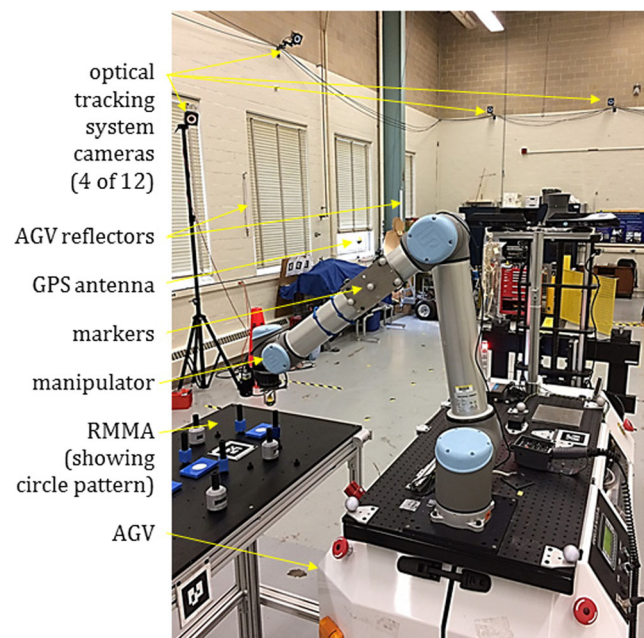


Fig. 1 Mobile Manipulator positioned next to the reconfigurable mobile manipulator apparatus (RMMA)

platform where the position and orientation (pose) of the mobile base relies on reflectors mounted on the surrounding walls or within the AGV world. The robot arm or manipulator is mounted on the AGV top-front. Cameras from an optical tracking system are mounted to the lab walls and used for measuring mobile manipulator pose. Additionally, an artifact that was developed at NIST, called the reconfigurable mobile manipulator artifact (RMMA), is used to measure the mobile manipulator by using a novel and relatively cost effective concept. Timing between the optical tracking system, AGV, and manipulator control computers is synchronized by using a global positioning system (GPS) antenna.

Measurement of the manipulator's Cartesian pose, which is combined with the mobile base's pose, is relatively complex as the system can include nine or more degrees of freedom. The RMMA is designed to simplify measurement by allowing the robot wielding a tool point sensor to trace various geometric patterns and to sense the dimensional points along the patterns. Two artifacts were designed and manufactured at NIST to include flat, rotated, convex and concave geometric patterns to trace to allow for three different mobile manipulator performance measurement scenarios. The three scenarios are described as: A) static: the AGV stops while the robot accesses all points within its work volume, B) indexed: the AGV initially stops while the robot accesses most points within its work volume, informs the AGV to increment to a new point, and to stop while the robot accesses the remaining points, and C) dynamic: both the AGV and robot simultaneously move while the robot accesses all points. This paper will discuss the B scenario as it includes aspects of all three scenarios of both mobile base and manipulator move, pose, and reposition.

Towards the main objective of this paper, to apply SysML modeling to the performance measurement of mobile manipulators, Fig. 2a shows a SysML package model of the described systems. This high-level drawing provides an overview of the systems that make up the mobile manipulator, the optical tracking measurement system with multiplicity of cameras and e.switches (Ethernet switches) shown. As shown in Fig. 2a, the RMMA includes one or many fiducial-reflector blocks that are used to make up patterns for the mobile manipulator to test against. Additionally, a bisect-fiducial block is shown and used for registration of the mobile manipulator to the RMMA. This high-level drawing will be detailed in the following sections describing each of the three packaged systems: Mobile Manipulator, Optical Tracking Measurement System, and Reconfigurable Mobile Manipulator Artifact.

The mobile base, as briefed in Section II, is an AGV manufactured with the industry's pseudo-standard controller and software [6] as shown in Fig. 2b as parts to the AGV

controller-offboard block. This example vehicle has many of the same components found in autonomous industrial vehicles with navigation sensors (Nav sensor) that may or may not require facility reflectors. If the vehicle uses simultaneous localization and mapping (SLAM), features of the facility would be shown in place of the Facility reflectors block. Steer and Drive motors and amplifiers, and batteries are also typical. In the experimental case provided in this paper, there is also an offboard manipulator controller (Manipulator controller-offboard) which may not be typical of industry as all manipulator control may be onboard.

However, it is essential that the independent AGV and onboard manipulator controllers communicate their relative poses, in this case to the artifact. There has been a lot of research in centralized and decentralized offboard robot-to-robot communication [7] and combined controller communication [8], although there is little discussion of combined, yet independently controlled, mobile base and manipulator control communication methods in the literature.

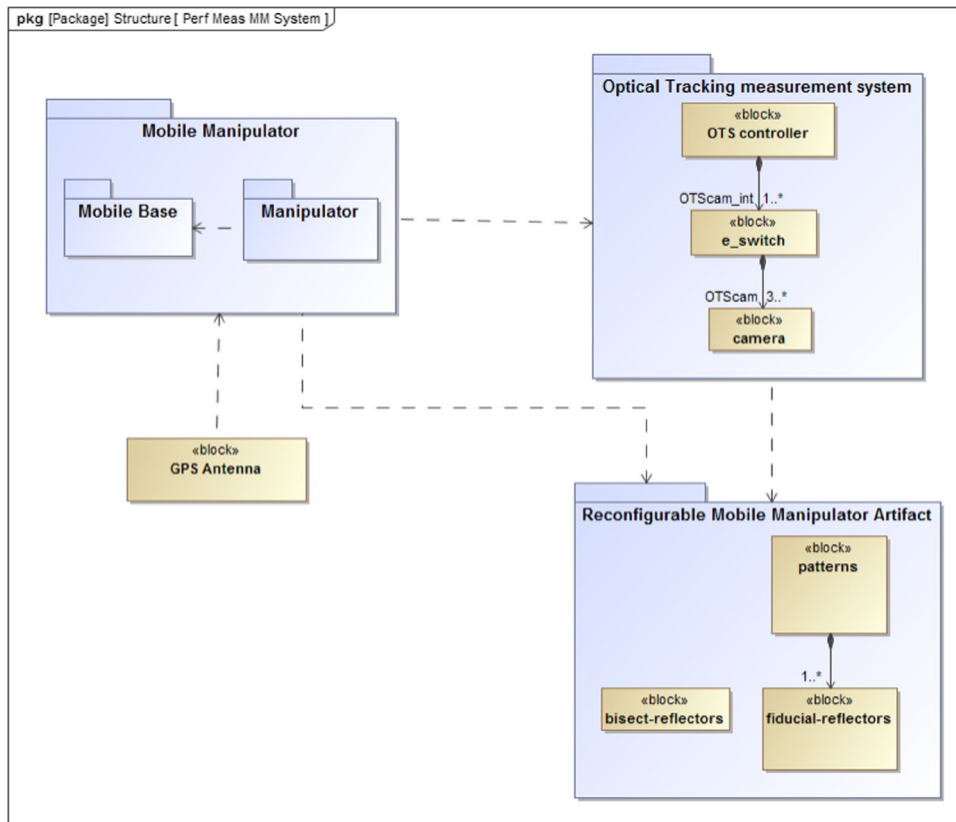
The manipulator internal block diagram shown on the right side in Fig. 2b has a similar component layout as for the AGV with motors/amplifiers, encoders, and an onboard and offboard controller. Additionally, an end-of-arm tool (EOAT) is included that carries a tool, which in this case is a laser retro-reflector. The Manipulator controller-offboard provides the connection to the onboard AGV controller (CVC600) and associated software parts are listed. A camera viewing augmented reality tags is included to show an alternative registration tool, although this is not the main focus of the paper.

2.1 Mobile Base

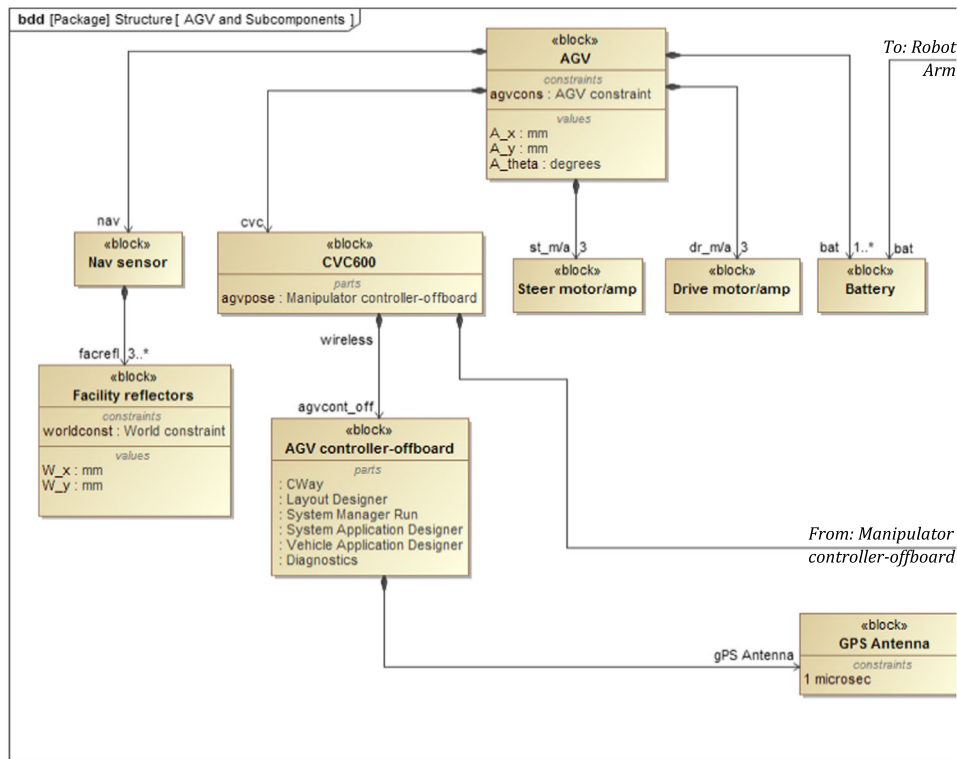
The internal block diagram shown in Fig. 3 models much of the same components as in the block definition diagram shown in Fig. 2b with the obvious addition of the Wheels and Encoders parts. However, this diagram also displays the types of signals that are passed between components. The diagram also shows signal flow direction stemming from ports attached to various parts.

2.2 Manipulator

The manipulator internal block diagram shown in Fig. 4a is different from the AGV internal block diagram because of the end-of-arm-tool which includes an additional constraint of tool positioning along with the base mounting constraint (Manipulator Base constraint). This part constraint describes the mounting uncertainty that can occur when the manipulator is mounted to the mobile base. And, although the AGV is linked to the Robot arm part due to the onboard manipulator mount, the AGV includes its



(a)



(b)

Fig. 2 SysML (a) package diagram and (b) left and (c) right side of the block diagram showing the mobile manipulator and measurement system structure. The same battery and GPS antenna are shown in both (b) and (c) to show their interconnections to both the AGV and Robot arm systems

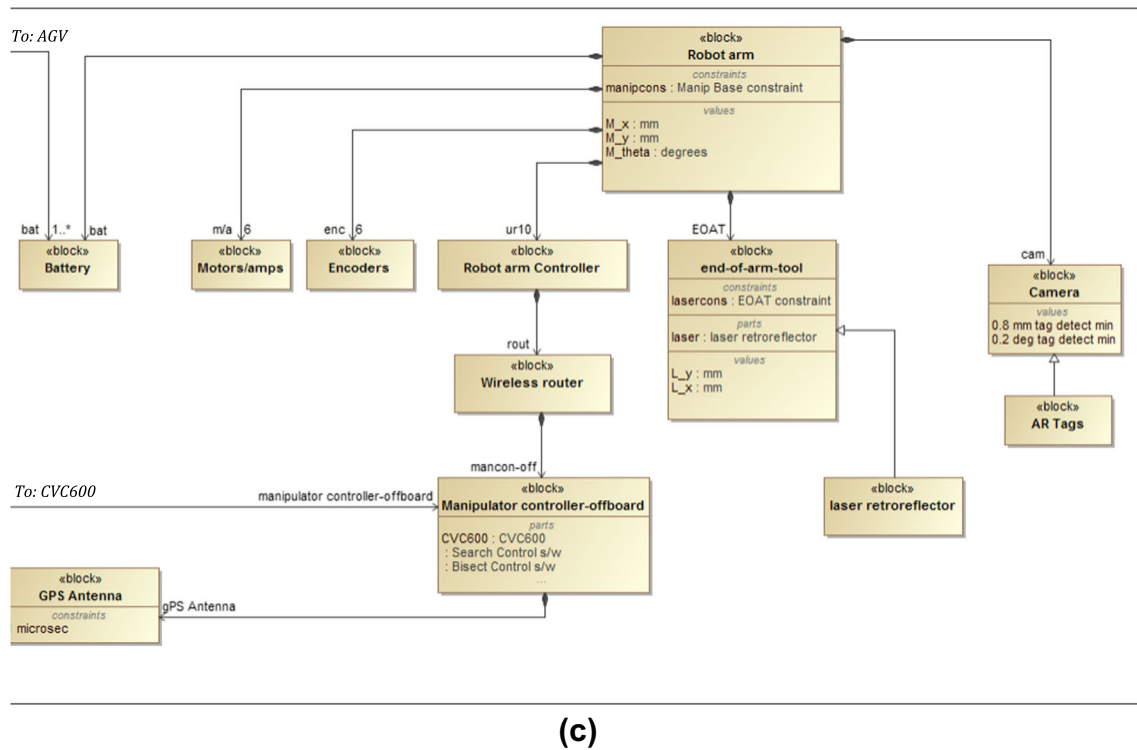


Fig. 2 (continued)

additional constraint of pose uncertainty. These will be further detailed in Section 4.

Figure 4b shows an internal block diagram of the algorithms that controls the manipulator during performance measurements. The manipulator control algorithm is relatively straightforward in its design where simple manipulator movements are intended during the performance measurement process. As such, a more generic methodology is shown and described here as would be the case in standards documents for this concept so that a particular design is not mandated. Figure 4b therefore, shows the dependencies of moving to particular locations, first to ensure appropriate communication, and second to ensure proper manipulator movements from one location to another and while at a particular location to fulfill the performance measurement objective.

On the lower right are one hardware part (CVC600) and two software parts from the AGV (System Manager Run and CWay). The manipulator is dependent upon the System Manager Run program informing the manipulator of the AGV pose when parked at the RMMA. The manipulator performs intermediate motions to two poses that cause the manipulator to approach the Bisect Control and Search Control registration points on the RMMA the same way. This ensures that the manipulator will not attempt to

pass the end-of-arm-tool through the base of the robot or other self-destructive motion at different AGV poses next to the RMMA. Dependent upon the operator selection of performance measurement type, either the bisect or search methods are performed. Step sizes for the Bisect Control are left variable allowing the operator to choose the time for the manipulator to bisect to find the large reflector center and/or the accuracy of the center. For example, a 0.25 mm step size will take much longer to find the reflector center versus a 2 mm step size which also includes much higher uncertainty. Similarly, when using only the Search Control for registration to the RMMA, a very small step size provides relatively higher accuracy. However, a step size of half the diameter of fiducial reflector was determined an ideal step size. For example, when 1 mm fiducial diameters were used, the 0.5 mm step size was used. Based on the AGV location, one of two patterns are then traversed. Stowing the manipulator was programmed to occur when the pattern was completed or when performing Bisect Control or Search Control that did not produce appropriate results within a chosen time period. For example, if the Bisect Control did not initially result in a reflector detect or if the Search Control took more than 200 steps, the manipulator Stow function was executed and the AGV System Manager Run program was alerted that the AGV could move.

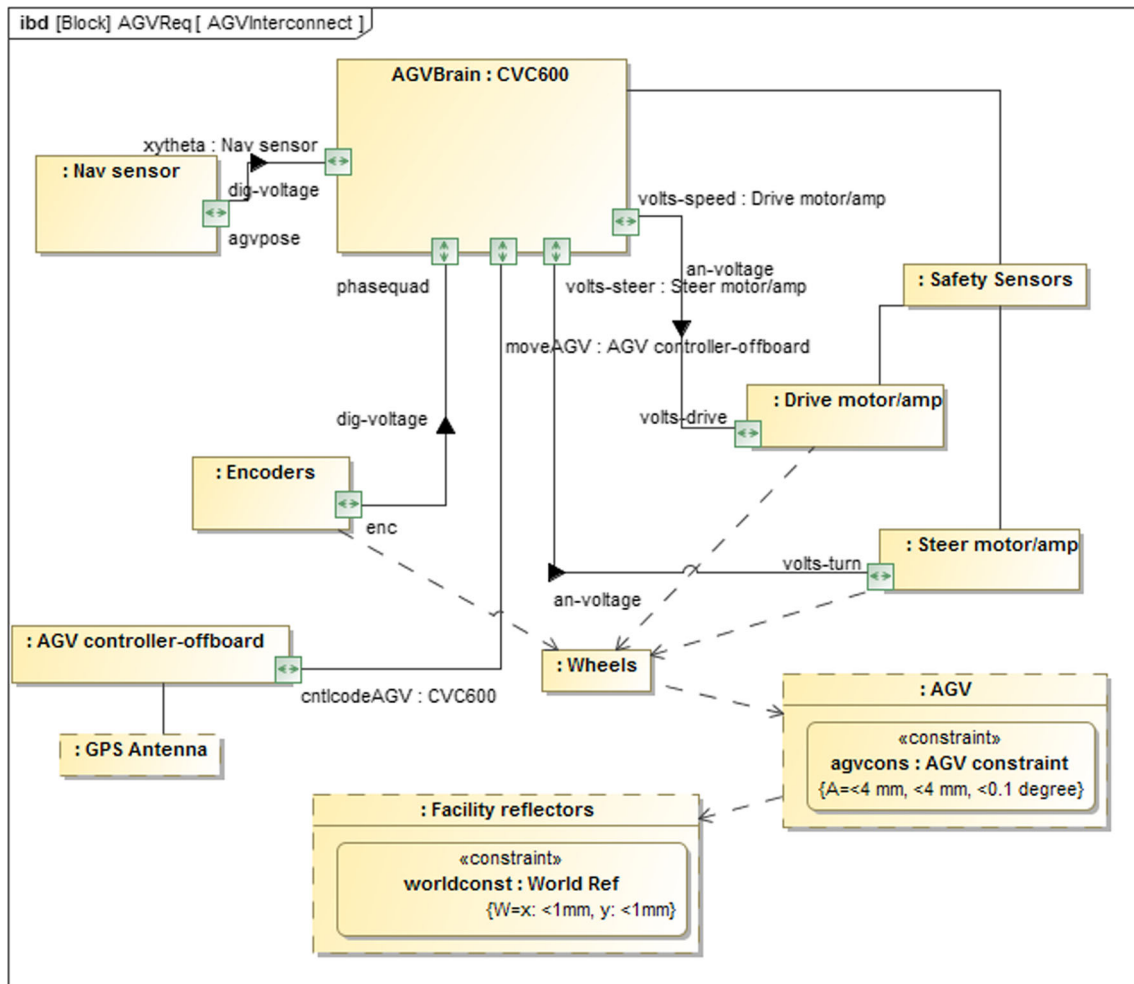


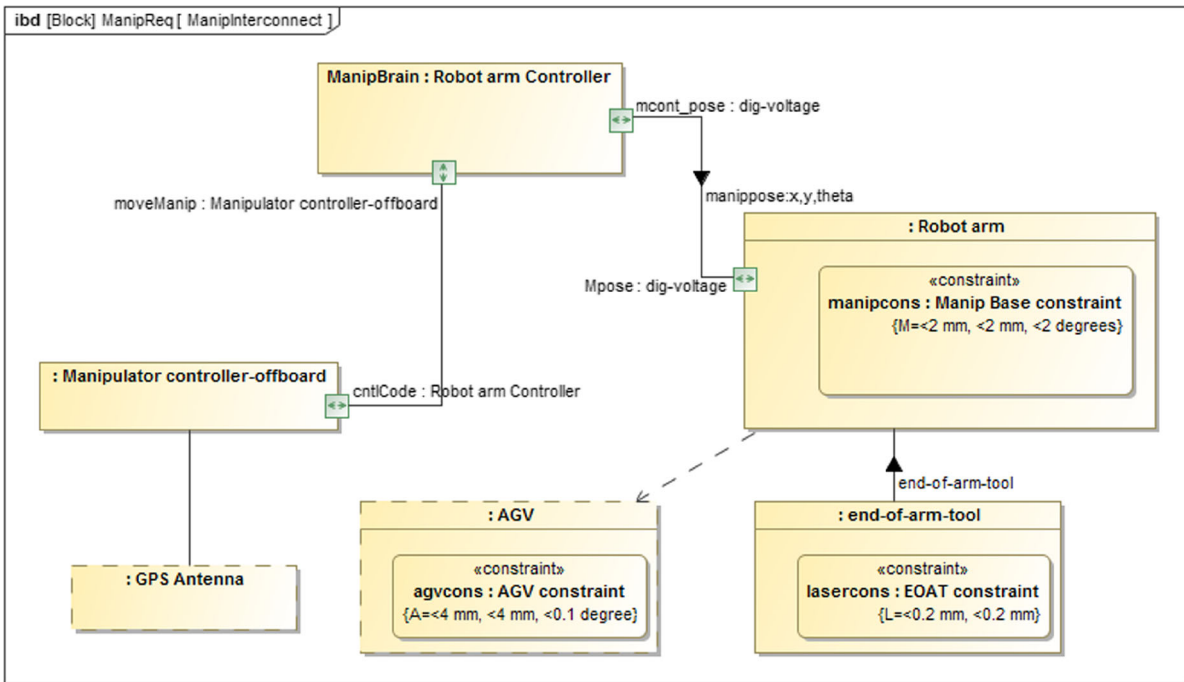
Fig. 3 SysML internal block diagram of the mobile base (AGV) and subcomponents

3 Performance Measurement Systems

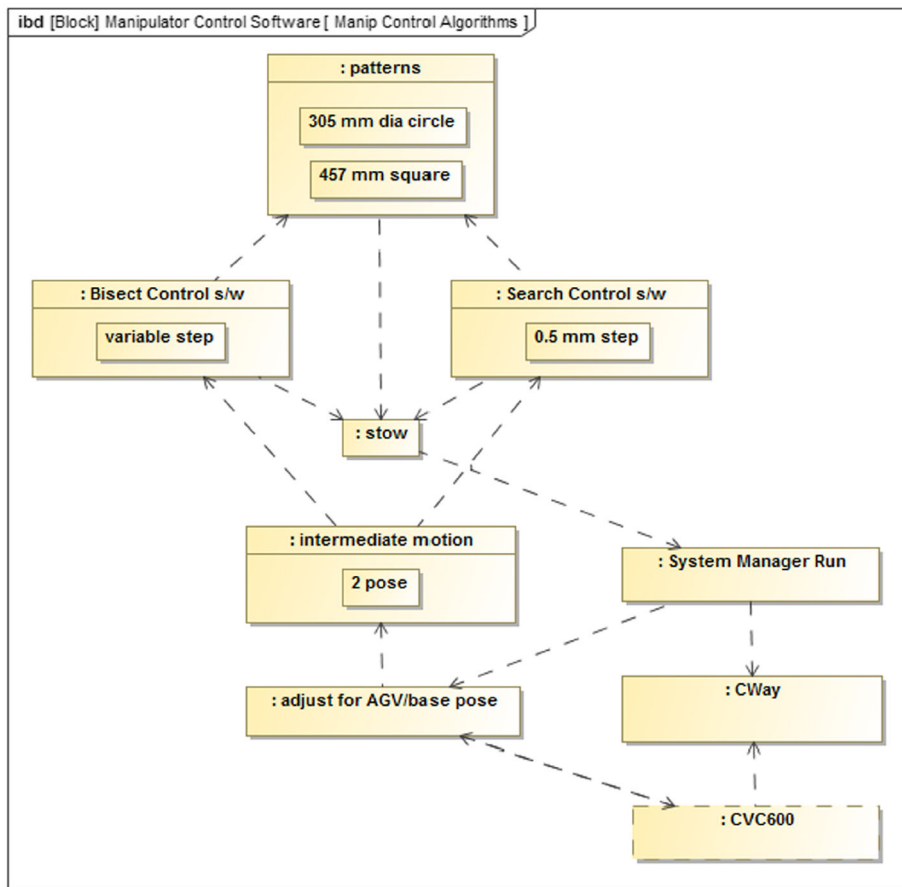
Metrology methods for measuring performance of mobile manipulators, with technologies used to access parts or assemblies in manufacturing processes, include: physical contact using a touch probe [9], cameras detecting fiducials [10, 11], laser interferometry [12, 13], theodolites [14] and coordinate measuring arms [15]. An example of uncertainty (position accuracy) for the camera calibration system in [11] was 0.1 mm and 0.2 mm for 650 mm and 950 mm target distances, respectively. Other metrology methods in accordance with ISO 9283 [16] include: Path comparison, Trilateration, Polar coordinate measuring, Triangulation, Optical tracking, Inertial measuring, Cartesian coordinate, and Path drawing.

This section provides information and SysML models of the two methods we have chosen for measuring performance

of mobile manipulators: optical tracking measurement systems and artifacts. Both methods are useful and provide promising results. Using SysML to describe the two measurement systems provides a simple, yet dramatically different view of how they function. The optical tracking system model shows an active, computer controlled and electrically interconnected system of components. Whereas, the artifact measurement method shows a much more passive (except for the laser) concept that uses a variety of reflectors to accomplish similar mobile manipulator performance measurement. Due to the complex motion of the dual system (AGV and robot arm), we chose the optical tracking system of multiple cameras with a large combined field-of-view. Second, we chose to develop an artifact that could, by comparison to the optical tracking system, potentially prove cost effective while providing the desired maximum uncertainty for mobile manipulator performance measurement.



(a)



(b)

Fig. 4 SysML internal block diagrams of the (a) physical manipulator (Robot arm) subcomponents and (b) the control software components

3.1 Optical Tracking Measurement System

Figure 5 displays a SysML internal block diagram showing the optical tracking measurement system structure. The controller (OTS controller), as with the AGV and manipulator controllers, was also time-synchronized at $1 \mu\text{s}$ with GPS through an antenna. This optical tracking system included 12, 4 MP (megapixel) cameras attached to the controller via Ethernet through two hubs (EthHub1 and EthHub2) and through an Ethernet switch (e_switch), all with 1000 MB maximum data flow capacity. An external timesync shown in the figure is also available and was not used for these experiments. Experimentation has demonstrated that this optical tracking system used for measuring performance of the mobile manipulator described in this paper has a static measurement uncertainty of 0.022 mm and 0.046° and dynamic measurement uncertainty of 0.26 mm and 0.20° [17].

3.2 Reconfigurable Mobile Manipulator Artifact

An alternative to the measurement system referenced previously and the optical measurement system modeled in Section III-A is the use of artifacts. Bostelman, et al describe in [18] the use of a novel artifact standardized in ASTM E3064-16 [19] and used as in the test method for measuring optical tracking system performance. Similarly, NIST developed an artifact, called the reconfigurable mobile manipulator artifact (RMMA), expected for use within a standard test method to measure the performance of static manipulators and mobile manipulators. By comparison, it is estimated that the use of the RMMA could be 20 times lower cost than the use of the described optical tracking system. In this case, the RMMA is a metal plate with fiducial mount points at precise locations. The RMMA, shown in Fig. 1 beside the mobile manipulator, could also be made using additive manufacturing and as estimated, further reduce costs by another

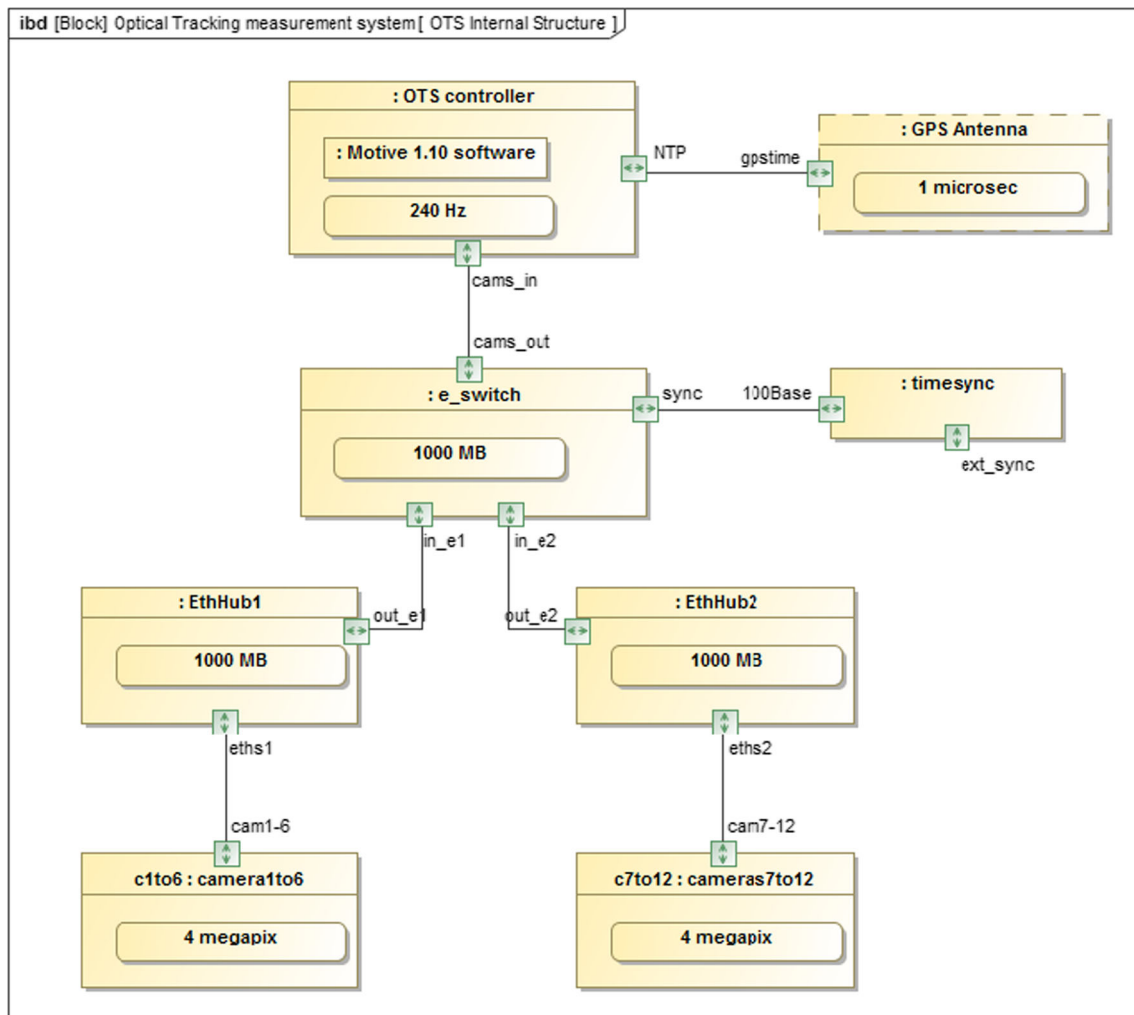


Fig. 5 SysML internal block diagram showing the optical tracking measurement system structure

order of magnitude. Reflective fiducials are to be detected using a laser retroreflector detector, carried by the manipulator as the EOAT, passing through a collimator attached to the RMMA. A 305 mm (12 in) diameter circle pattern and a 457 mm (18 in) square pattern of fiducials are machined with 0.025 mm (0.001 in) tolerance into the RMMA. Other components are also part of the RMMA where all components are modeled in a SysML internal block diagram shown in Fig. 5.

Beginning at the laser retroreflector (Fig. 6, bottom-left), a positioning constraint is applied to the EOAT provided by the robot manufacturer specification. Moving up the left of the model, the collimator has a 13 mm inside diameter limiting the EOAT angle relative to the RMMA where fiducial detection can occur. The collimator is attached to two different types of fiducial reducers ('fid-refl-reducer-fixed' with a fixed reflector diameter 2 mm or greater, depending on the EOAT uncertainty chosen, and a 'fid-refl-reducer' with a variable reflector diameter of 1 mm or

greater that uses an optical aperture to minimize diameter to the center of the reflector). Both of the fiducial reducers are above 10 mm square fiducial-reflectors and attached to the RMMA through surface connectors into circle and square patterns embedded in the machined surface of the RMMA.

Since the mobile manipulator may or may not already be registered to the RMMA. The Fig. 6-left modeled parts can be used for mobile manipulator registration with the RMMA using search methods where the fiducial locations are previously taught. A second set of parts is also modeled (Fig. 6-center) showing the laser retroreflector being used to detect 42 mm diameter reflectors (bisect-refl-reducer) for an alternative mobile manipulator-to-RMMA registration method. The 42 mm diameter was chosen so that the EOAT would always detect these reflectors and a control method, called bisect and described in Section 4. Model Verification, could be used for the registration process. Off-the-shelf 50 mm x 80 mm rectangular reflectors (bisect-reflectors)

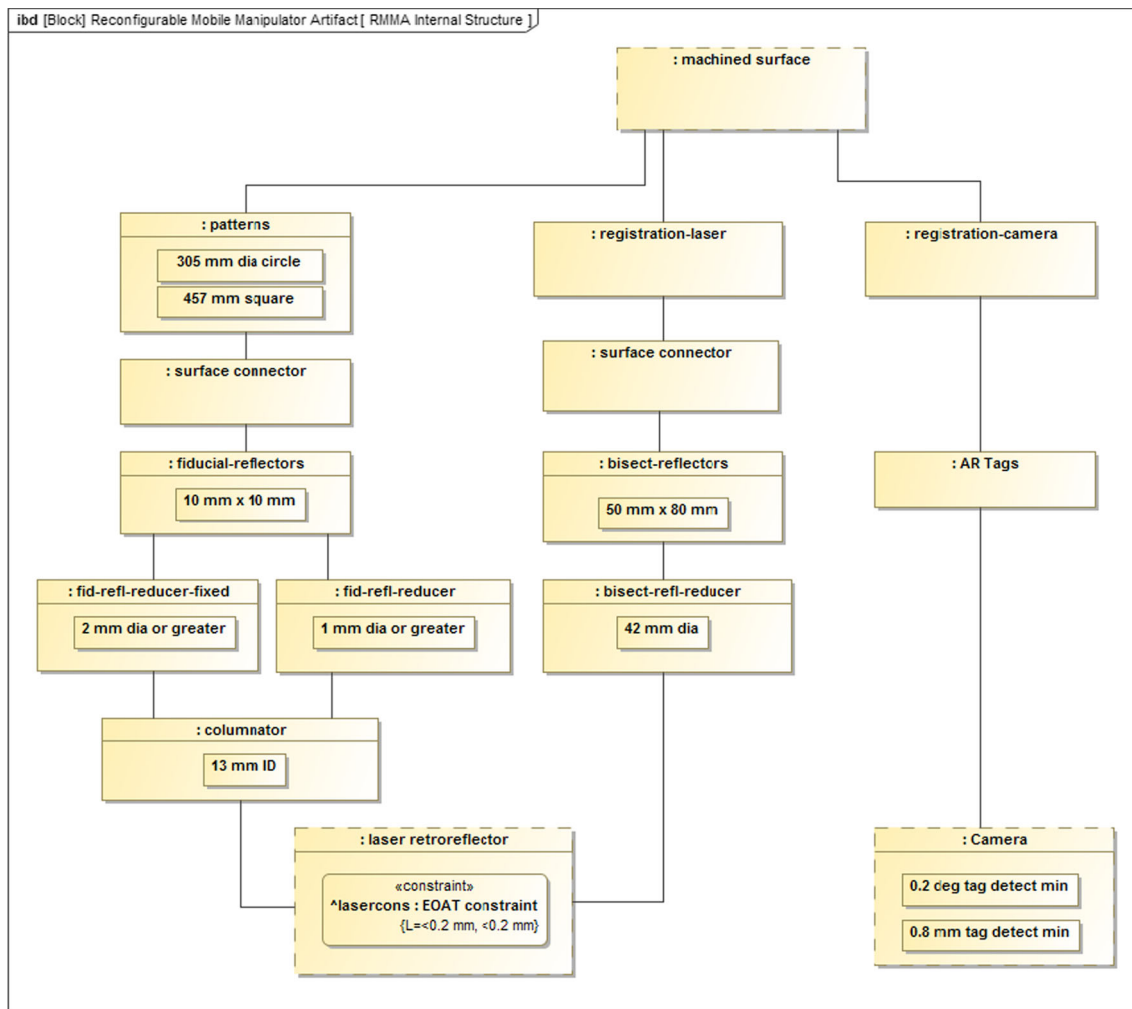


Fig. 6 SysML internal block diagram showing the reconfigurable mobile manipulator artifact (RMMA) structure

were covered by the bisect-refl-reducer and mounted to the RMMA using surface connectors at initially taught manipulator locations (registration-laser) on the machined surface.

A third, parallel RMMA structure was modeled (Fig. 6-right) showing a camera that detects augmented reality tags (AR Tags) with 0.2° and 0.8 mm tag detection capability using the AR Toolkit software and calibration as described in [21]. The method provides a third alternative to the two laser retroreflector registration methods previously described. Although to the date of this paper, this third method has not been verified for uncertainty as a useful registration method for performance measurement of mobile manipulators and is therefore, left for future research.

4 Model Verification

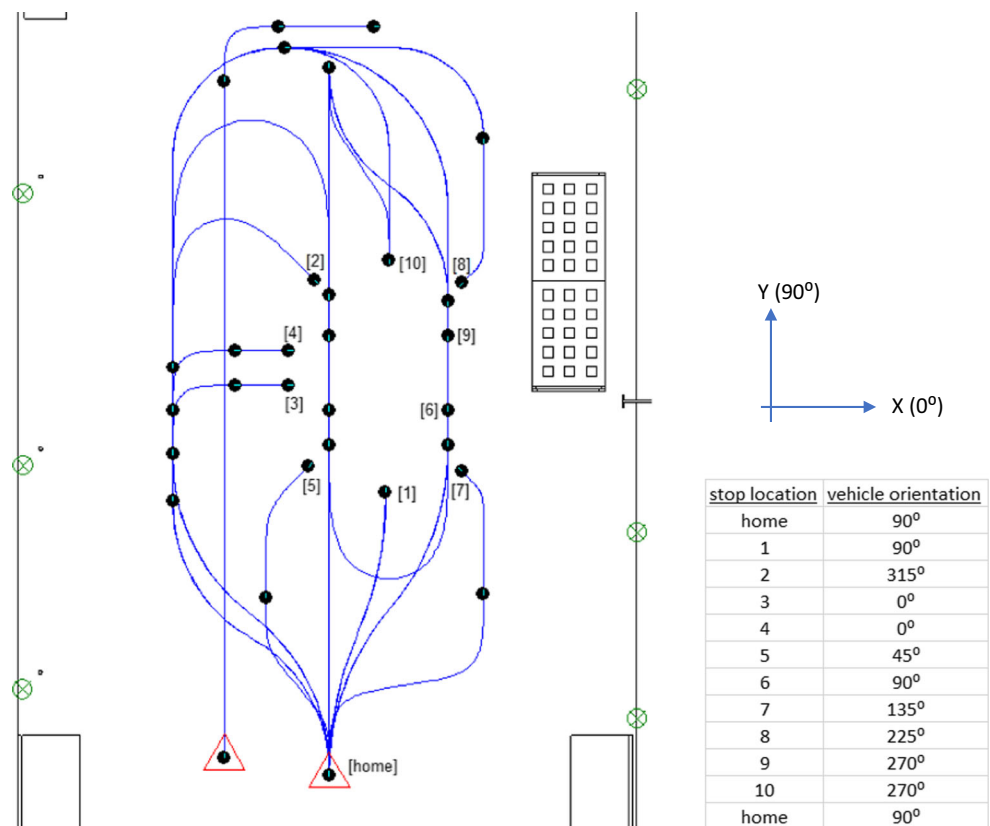
As noted in Section 1, previous experiments have been performed that validate the SysML models described in this paper. A mobile manipulator performance measurement concept was developed over the past two years [20–22]. This concept, which expanded on the experiments in [20], consisted of using a NIST-developed, reconfigurable mobile manipulator artifact (RMMA) (see Fig. 1) with varying-sized fiducials to be detected by a sensor carried by the mobile manipulator to minimize the measured uncertainty.

The AGV control program pre-programmed the fork-style AGV movement to 10 different (see Fig. 7) poses. AGV orientation angles were programmed to be at 45° increments with respect to the RMMA. The AGV moved from a home position away from the RMMA to the first pose next to the RMMA, stopped and waited until the manipulator registered to RMMA bisect reflectors and then detected a pattern of fiducials mounted in a circle and a square pattern.

Upon completion of the circle or square pattern fiducial detections for one location, the AGV moved to the second location and pose, and so forth until ten locations were completed. The AGV completed the test by moving to the home position.

A laser retroreflector was mounted perpendicular to the manipulator end-of-arm-tool joint and used as a reflector detection device. A circle pattern and a square of 2 mm diameter fiducial reflectors were mounted to the RMMA. Additionally, two large, 42 mm diameter “bisect” reflectors were mounted within the two patterns (i.e., four total) and used as registration reflectors for the mobile manipulator. The size of the bisect reflectors was chosen to ensure that with the mobile manipulator uncertainty, it would always initially detect these registration reflectors for each pose. A “bisect-with-search” registration method for registering the mobile manipulator to the RMMA was developed. Once the registration was completed, the mobile manipulator was expected to then detect all fiducials within a local pattern

Fig. 7 **a** Map of AGV reference point paths (blue lines) and stop points (black dots on paths), and approximate locations of AGV wall-mounted reflectors (green circles with Xs) used for navigation. **b** Table of AGV stop locations corresponding to the map and vehicle orientation at each stop location with reference frame above the table. The left, straight-to-right turn path that begins at the unmarked home triangle was not used



(circle or square) and at the current AGV pose. Upon completion, the manipulator stowed and the AGV moved to the next pre-taught pose until all 10 poses were completed.

The Mobile Manipulator program was developed at NIST and controlled the manipulator during the tests. It interfaced with the AGV onboard controller directly to obtain the current AGV pose, and it interfaced with the NIST-developed, AGV control program running on the off-the-shelf, Order Manager application to coordinate the motion of the arm with the motion of the AGV. The AGV control program signaled the Mobile Manipulator program when it arrived at one of the stop or test locations. The AGV control program also sent the identification number of the test location. The Mobile Manipulator program read the current AGV pose and used it to compute the initial search location of the two registration reflectors in the target pattern (circle or square). Additional patterns could also have been used in the Mobile Manipulator program and would be encouraged for thoroughly testing mobile manipulator performance during factory implementations.

When the AGV was stopped at the RMMA, the manipulator was first moved from a stowed location to the first of the two registration reflectors, performed a bisect search for the reflector center and moved to the second reflector to repeat. When the locations of the two registration reflectors were determined, the program had sufficient information to compute the locations of the other fiducials in the square or circle patterns. For comparison to repeatability, the initial registration number of iterations count was logged and included in results.

Once the locations of all reflectors in the pattern were computed, the manipulator cycled through them a set number of times – one time for the circle and two times for square patterns. At each fiducial reflector, the laser retroreflector checked to see if the manipulator was aligned with the reflector. When the test was completed, the manipulator was moved to the stow location and the Mobile Manipulator program signaled to the AGV control program that it was clear to move.

The positions of the circle and square patterns of fiducials were recorded prior to performing the repeatability tests. The AGV was first moved to a location where it could reach both of the patterns of fiducials. The current location and orientation of the AGV was recorded. The arm was repositioned manually with the robot teach pendant until the sensor detected alignment with each of the index fiducials, and the manipulator position was recorded. This information, along with the manipulator base position relative to the vehicle's coordinate system, allowed the correct manipulator coordinates for the index fiducials to be calculated for an arbitrary AGV location. This allowed the AGV to approach the RMMA from any direction and to compensate for variation in the AGV's stopping pose.

The calibration of the manipulator base location involved recording the position of one or more fiducials from a variety of locations. Both the AGV location and the manipulator coordinates of the fiducials were recorded. This data was processed using an iterative, non-linear model to find the best value of the manipulator base pose.

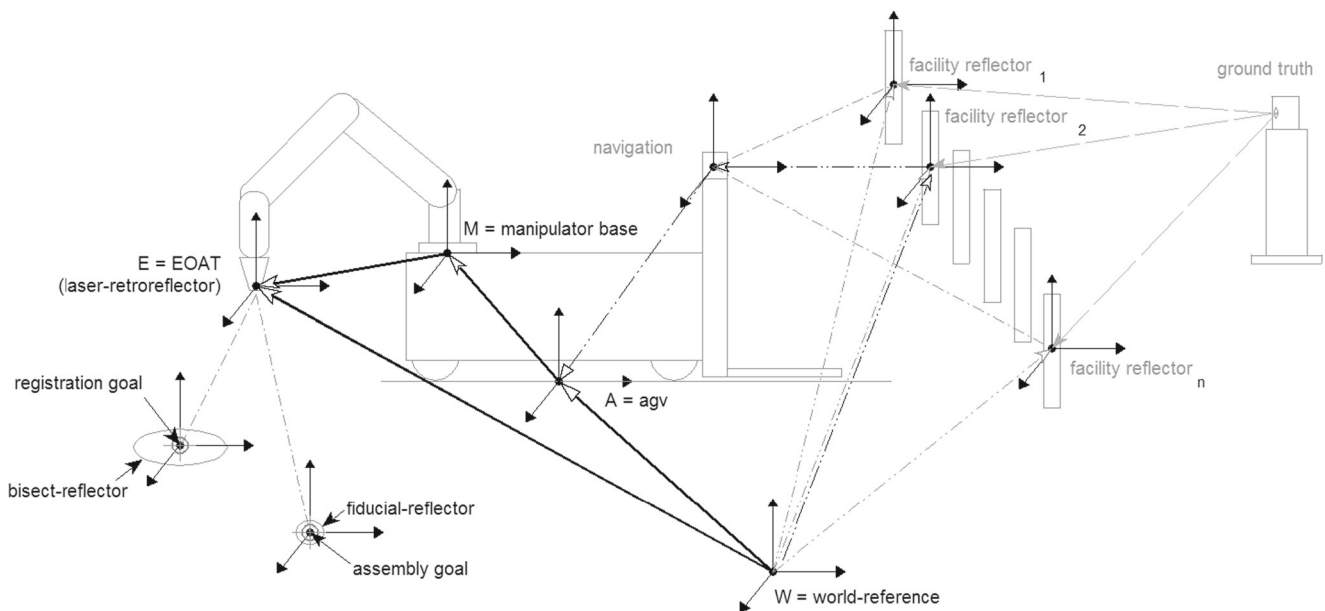
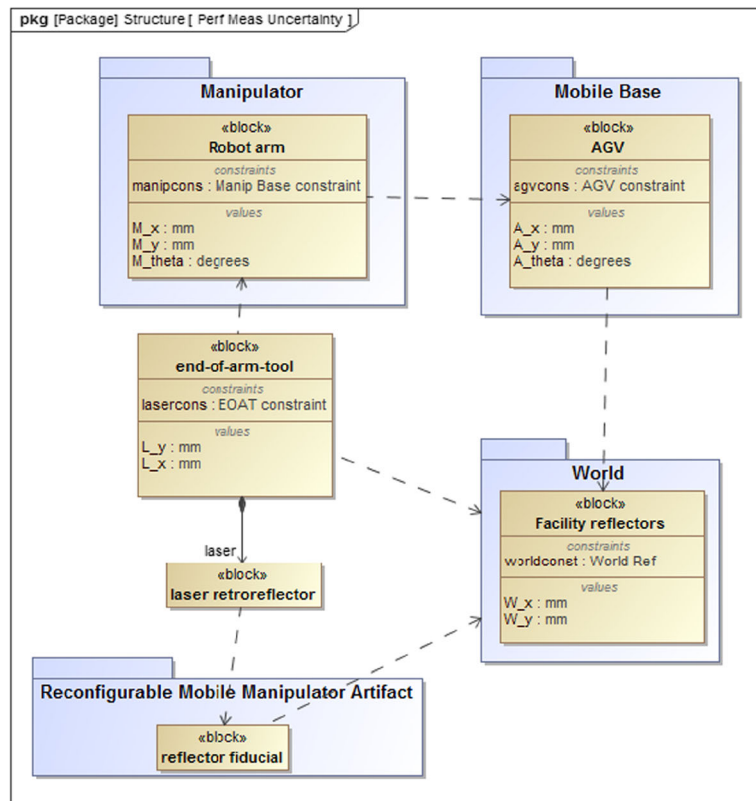
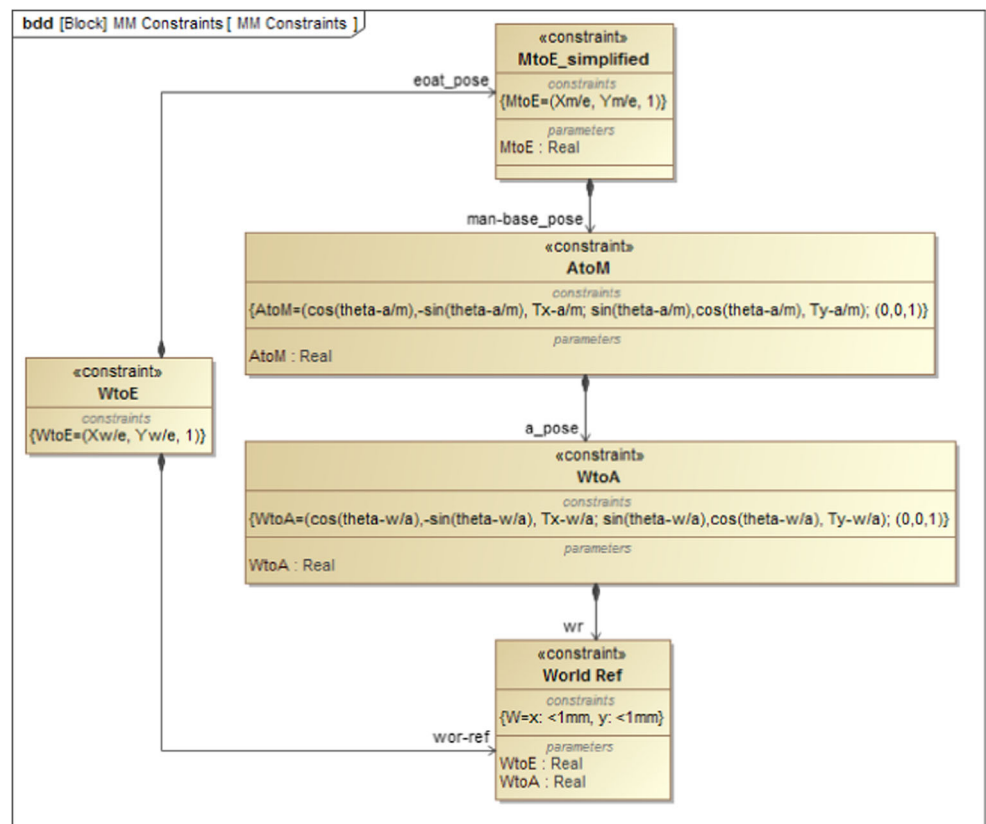


Fig. 8 Drawing showing the uncertainty propagation for performance measurement of a mobile manipulator

Fig. 9 SysML (a) package diagram showing the mobile manipulator and RMMA components that add to performance measurement uncertainty and (b) block definition diagram showing the constraints for the AGV, Manipulator Base, and EOAT that reference to the World constraint



(a)



(b)

5 Uncertainty Propagation

As a preliminary notion, the world, within which a mobile base such as an AGV, should be measured and provided to the vehicle controller as reference. The vehicle pose will only be as accurate as its reference. Similarly, it has been shown in previous research [23] that an AGV approaching the same point from various directions is relatively inaccurate as compared to approaching the point from one direction. Therefore, AGV calibration is essential to enable higher accuracy and repeatability for the mobile manipulator which references the robot base pose to the mobility system or AGV. Figure 8 shows a drawing of the mobile manipulator, its reference to the world through facility reflectors, and the performance measurement concept of using a laser-retroreflector carried by the manipulator to register to reflectors. When compiling the three vectors from the world to the AGV to the manipulator base and to the laser, a propagation of uncertainty [24] equates to a vector that simply points from the world to the laser as shown in the figure.

A typical method of measuring reflector locations in the world is to use a metrology system, such as a surveyor’s tool (i.e., approximately 1.5 mm uncertainty over 1.5 km [25]) or a laser tracker (i.e., approximately 18 μm uncertainty over 12 m [13]). The authors chose the laser tracker so that the AGV reference to the world would be relatively more accurate. An onboard, spinning, navigation laser range and azimuth sensor then provides pose information to the vehicle controller. One issue (i.e., first major uncertainty point (AGV)) with the AGV control is that it uses the measured pose with respect to the world (facility reflectors) and the AGV control reference location is at floor level, at the vehicle centroid (i.e., beneath the vehicle). As such, this location is very difficult to use as a measurement reference.

The robot arm is mounted on a machined breadboard with 50.8 mm spaced, threaded holes and the robot arm is mounted to the breadboard with a machined interface plate. There is some uncertainty as to how accurately the breadboard is mounted with respect to the AGV reference point and causing a second uncertainty point (Manipulator Base). The third uncertainty point is the relative accuracy of EOAT pose of the carried laser that the robot arm is capable of providing.

Initially, it is important to model the variables of each system that provides uncertainty. Figure 9a shows, using SysML package diagram, blocks within packages of the world, mobile base, manipulator, and the RMMA for their associated components. Additionally, the end-of-arm-tool which carries the laser retroreflector is shown. The links between each of the blocks mimics the drawing in Fig. 8 with the addition of a link from the RMMA to the world which, for verification of the RMMA location, was also measured with respect to the world reference frame used by the AGV. Within each block, values and constraints are also shown.

Each of the constraint labels (i.e., World, AGV, Manipulator Base, and EOAT constraints) can then be modeled in a block definition diagram, as shown in Fig. 9b, that allows each of their constraint parameters to be clearly displayed. Also, the parameters for each of the constraints is shown and the interconnect, that mimics the uncertainty propagation previously described, are also shown with the AGV, Manipulator Base, and EOAT all connected to the World constraint. This block definition diagram of constraints provides the basis for the parametric diagram shown in Fig. 10. The parameters for each of the constraints and interconnects that produce the uncertainty propagation are shown in Fig. 9b which can be described in the matrix equation:

$${}^wP_E = {}^wH_A * {}_A H_M * {}_M P_E \tag{1}$$

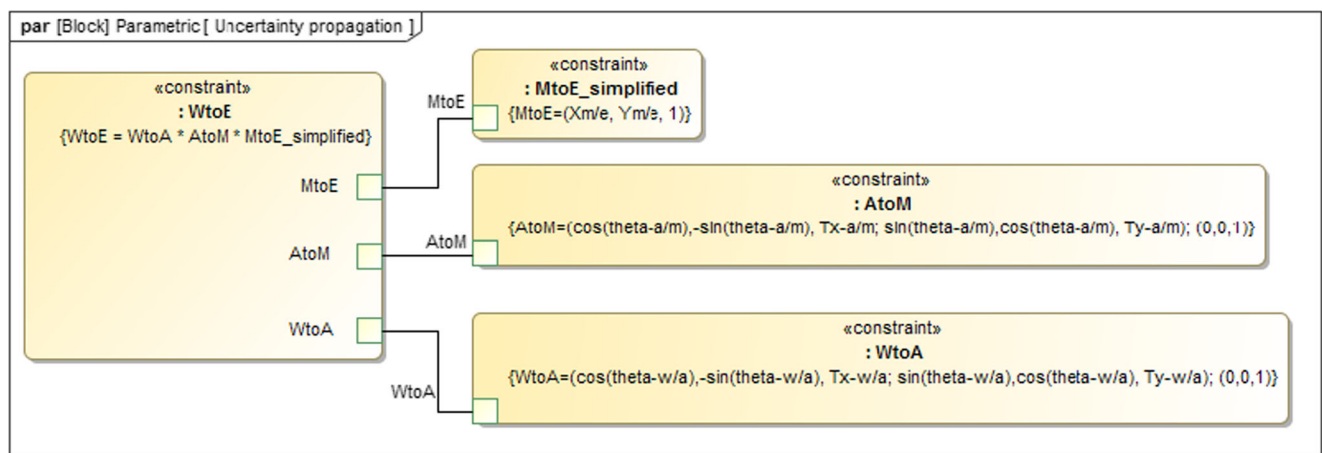


Fig. 10 SysML parametric diagram showing the uncertainty propagation for a mobile manipulator

or

$$\begin{pmatrix} X_E^W \\ Y_E^W \\ 1 \end{pmatrix} = \begin{pmatrix} \cos O_A^W & -\sin O_A^W & T_{X_A^W} \\ \sin O_A^W & \cos O_A^W & T_{Y_A^W} \\ 0 & 0 & 1 \end{pmatrix} \begin{pmatrix} \cos O_M^A & -\sin O_M^A & T_{X_M^A} \\ \sin O_M^A & \cos O_M^A & T_{Y_M^A} \\ 0 & 0 & 1 \end{pmatrix} \begin{pmatrix} X_E^M \\ Y_E^M \\ 1 \end{pmatrix} \tag{2}$$

$$\begin{pmatrix} X_E^W \\ Y_E^W \\ 1 \end{pmatrix} = \begin{pmatrix} \cos O_A^W & -\sin O_A^W & T_{X_A^W} \\ \sin O_A^W & \cos O_A^W & T_{Y_A^W} \\ 0 & 0 & 1 \end{pmatrix} \begin{pmatrix} X_E^M \cos O_M^A - Y_E^M \sin O_M^A + T_{X_M^A} \\ X_E^M \sin O_M^A + Y_E^M \cos O_M^A + T_{Y_M^A} \\ 1 \end{pmatrix} \tag{3}$$

$$\begin{pmatrix} X_E^W \\ Y_E^W \\ 1 \end{pmatrix} = \begin{pmatrix} \cos O_A^W (X_E^M \cos O_M^A - Y_E^M \sin O_M^A + T_{X_M^A}) - \sin O_A^W (X_E^M \sin O_M^A + Y_E^M \cos O_M^A + T_{Y_M^A}) + T_{X_A^W} \\ \sin O_A^W (X_E^M \cos O_M^A - Y_E^M \sin O_M^A + T_{X_M^A}) + \cos O_A^W (X_E^M \sin O_M^A + Y_E^M \cos O_M^A + T_{Y_M^A}) + T_{Y_A^W} \\ 1 \end{pmatrix} \tag{4}$$

where: P represents a 2D point, H represents a 2D homogeneous matrix, W = World, E = EOAT, A = AGV, and M = Manipulator. A SysML parametric diagram, not included here, can then be used to further display the equations within a model. If the RMMA were to be tilted to an angle other than parallel with the manipulator base, the point ${}_M P_E$ would change to a 3 x 3 homogeneous matrix ${}_M H_E$. Similarly, if the AGV reference was not parallel with the world reference, ${}_W P_E$ would change into a 3 x 3 homogeneous matrix ${}_W H_E$. In our case, the robot base height above the floor is relatively equal in height to the RMMA height thereby eliminating the need to include z in calculations.

The parametric diagram describes the mathematical equation of the uncertainty propagation transformation from the world to AGV, the AGV to the manipulator base, and manipulator base to the laser. Because of the difficulty to measure from the AGV reference location to the manipulator base ${}_A H_M$ and from the world reference to the EOAT ${}_W P_E$, they are considered unknowns.

6 Use Case of the Performance Measurement Methods

Up to this point, the mobile manipulator system and the measurement systems have been modeled, including the uncertainty propagation that can occur from performance measurements. SysML models are therefore needed to show how this information would be useful when applying

the mobile manipulator performance measurement concept. Three models are therefore, needed to explain the measurement concept: 1) an activity diagram that shows activity flow that occurs during performance measurement, 2) a sequence diagram to show the sequence of events that occurs during the measurements, and 3) a use case diagram that shows the tasks that are necessary during the application.

Figure 11 begins with the Start performance test point in the upper left and flows through activities to the Stop performance test in the lower right. Upon Start, the base (AGV) is commanded to begin the performance measurement test. The base moves to the first pose at the artifact. If the move is incomplete, the base continues to move until it informs the manipulator that it has stopped at the RMMA. The manipulator then moves from stow to the initial registration position. Again, if the move is incomplete, the same manipulator moves until completed where the manipulator performs one of the registration types (search, bisect, or ARTag). Upon completion, the manipulator moves and aligns the laser retroreflector with assembly reflector (fiducial) until completion. The manipulator then stows and informs the base that it has stowed. If the AGV has not completed all ten poses, it moves to the RMMA at the next pose and once again informs the manipulator that the base has stopped at the RMMA. If the AGV has completed all ten poses, five poses at the circle and five poses at the square patterns, the base returns to the home position.

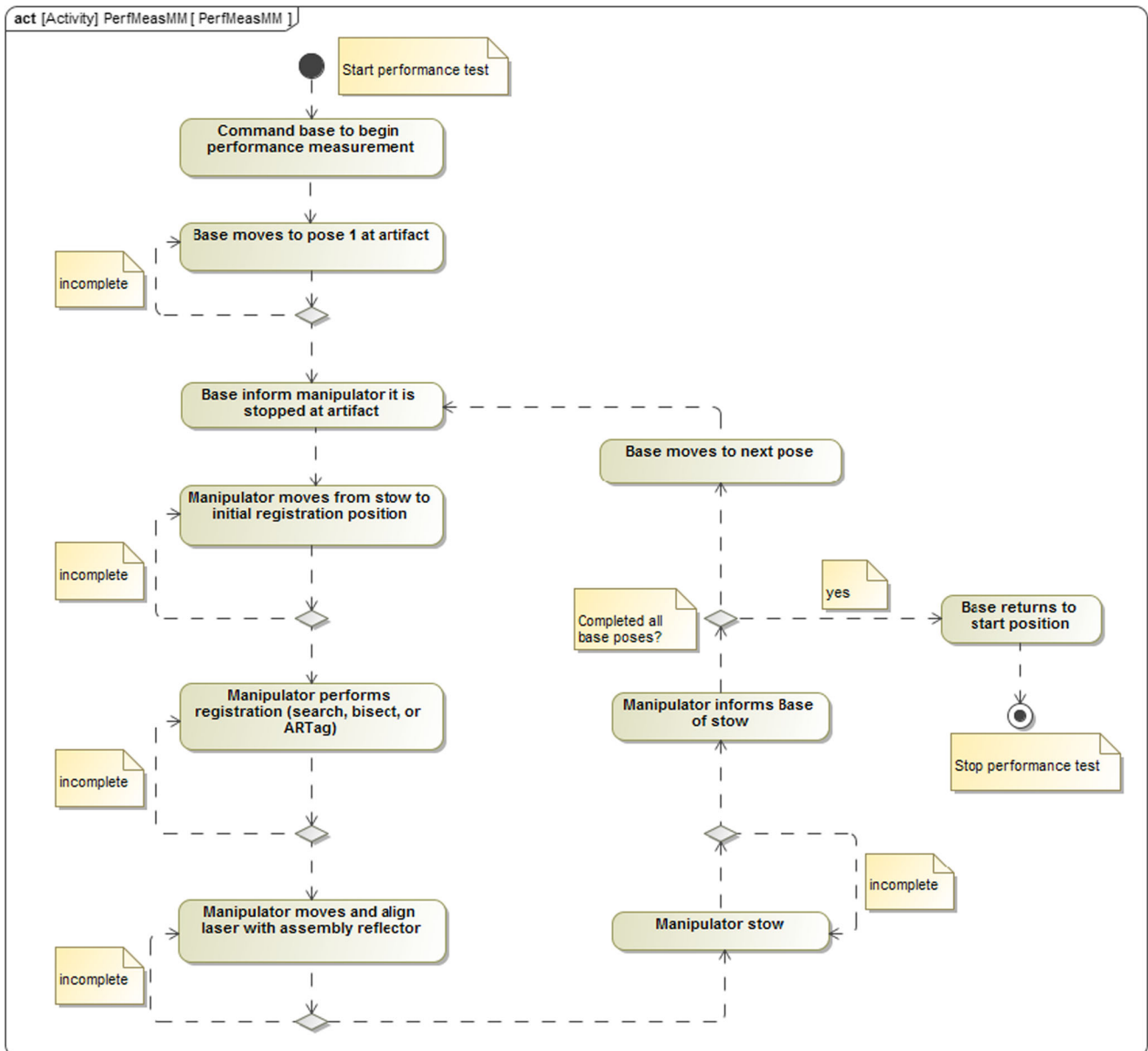


Fig. 11 SysML activity diagram showing the flow of activities for mobile manipulator performance measurement

The sequence diagram of events shown in Fig. 12 is read from top to bottom. The model shows eleven different sequential tasks beginning in the upper left by starting to measure using the optical tracking system. Next, the AGV offboard controller controls the AGV to begin movement towards the RMMA until it arrives and parks with a controlled pose at the artifact. Once parked, the AGV then informs the manipulator of the AGV arrival from the AGV onboard controller to the manipulator offboard controller. The manipulator is moved from the stow position and begins

a registration process to the RMMA. Upon registration, the manipulator then traverses through the set of fiducials associated with the pattern closest to the AGV parked pose. After traversal, the manipulator returns to the stow position, informs the AGV of the stow and that it's safe for the AGV to again begin motion. The AGV transport structure (control program) is incremented to the next pose and repeats until all ten poses have been completed. Upon completion, the optical tracking system stops tracking the mobile manipulator motion. The entire process combines both systems as an

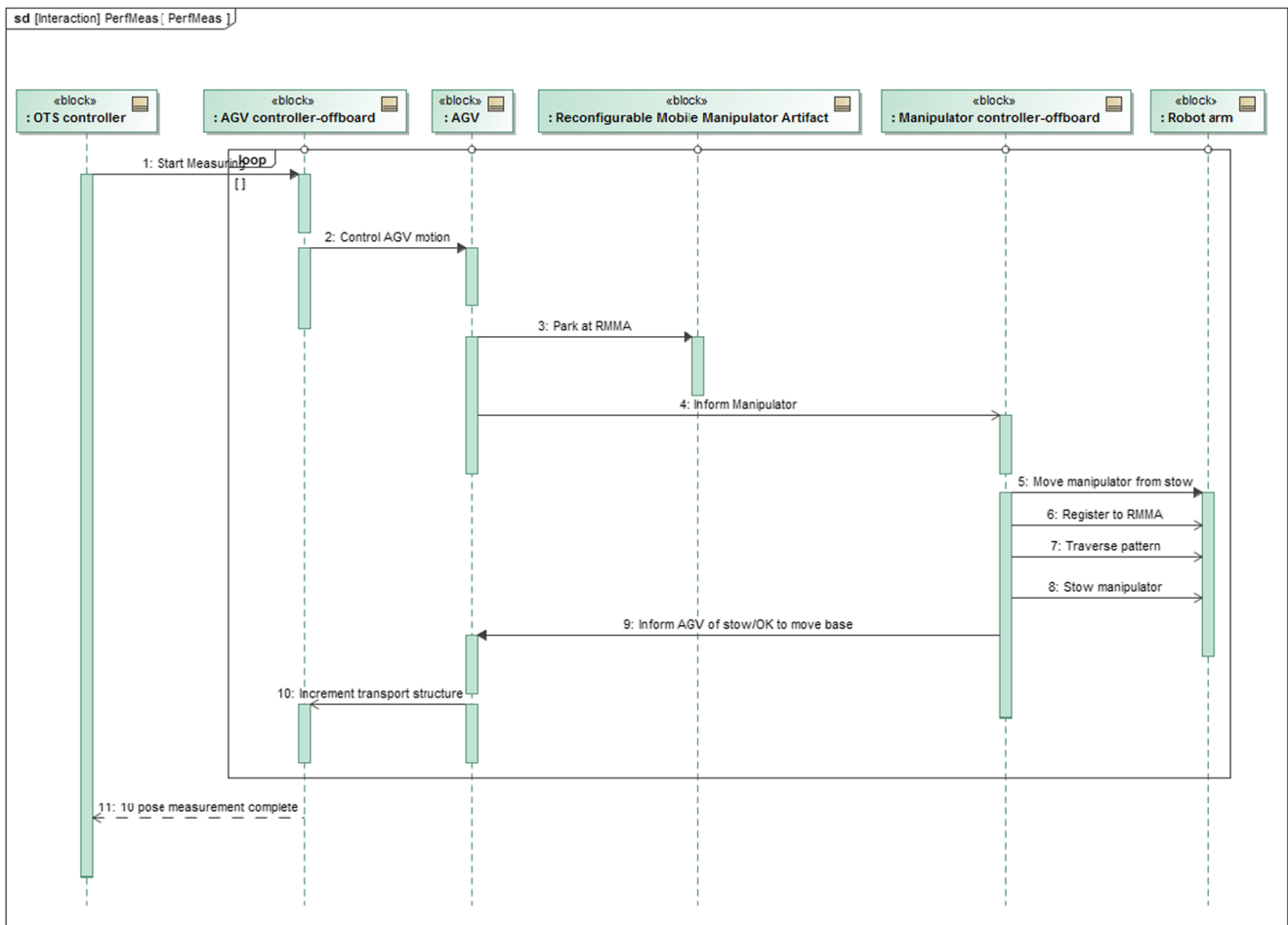


Fig. 12 SysML sequence diagram of mobile manipulator performance measurement using the RMMA

experimental comparison of the two methods. Ideally, only one method would be used. For example, if only the optical tracking system is used, the mobile manipulator may be programmed to move through a similar process as described although no registration to the artifact would be required. If only the artifact is used, no start and stop tracking of the optical tracking system would be required.

Figure 13 shows a SysML use case diagram modeling the process that represents a production facility where a mobile manipulator is: systematically sent from the production area to a calibration area (MM (mobile manipulator) System and Measurement Systems package), adjusted upon calibration (violet task), and then returned to ‘Continue normal production operations’. To be thorough, the addition of the three actors (with blue heads) were also needed to perform tests during the author’s experimental research. The parallel tracks for the optical tracking system (green tasks) and the use of the RMMA (yellow tasks) provide comparable methods.

Both systems, as explained in Section 3. B., are useful measurement methods and are dependent upon the stakeholder’s requirements for mobile manipulator accuracy and cost. One or the other would be chosen as the ideal measurement method while simplifying the use case models by removing method not chosen.

In the research use case, not only are the initial number of operators increased to perform the research experiments, there is no initial optical tracking power-on nor mobile manipulator power-on to steady state tasks and after adjustment of the mobile manipulator to peak performance, there is no return of the system back into production as is shown in Fig. 13. It is also expected that the ‘Adjust MM (mobile manipulator) parameters based on performance tests’ task would be performed automatically for the in-situ use case in Fig. 13 and may be either manually or automatically adjusted for the research experiment case.

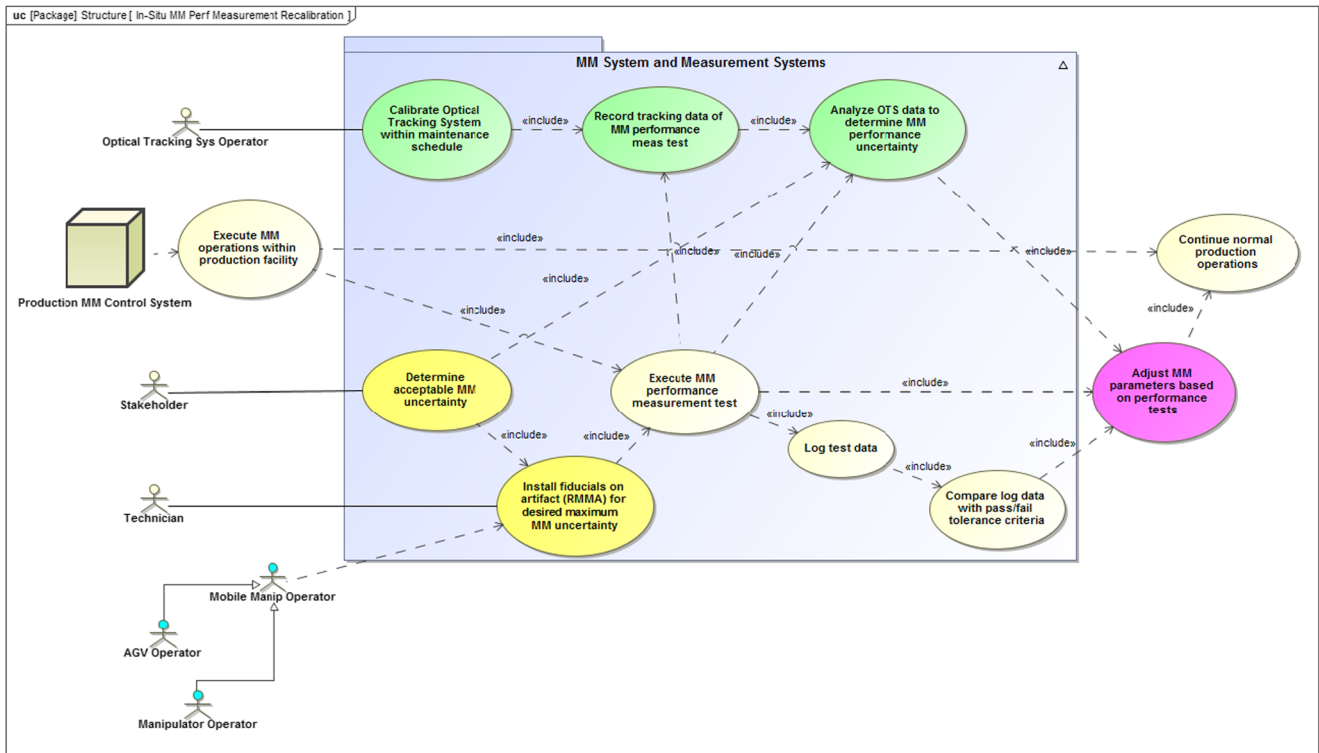


Fig. 13 SysML use case diagram of an optical tracking system (green tasks) in parallel with the RMMA (yellow tasks) used to measure performance of a mobile manipulator as may be found in a production facility during operation

7 Conclusions

Systems Modeling Language (SysML) is proven as a useful tool to model and generically show, in graphic form, performance measurement system for any mobile manipulator towards a standard format for this description. Should a different mobile manipulator be tested for performance than the one used for this paper, the models or portions of the models would simply be substituted for those shown in this paper and also proving the power of SysML.

Two measurement systems and methods were modeled: an optical tracking system also used as ground truth, and a novel artifact (reconfigurable mobile manipulator artifact or RMMA). Both systems are useful to measure mobile manipulator uncertainty. However, required setup, needed resources (personnel and cost), and uncertainty measurement requirements may sway the user to use one method over the other. Nevertheless, the research described in this paper and validated through experimentation showed a potentially useful artifact method that requires minimal setup, is cost-effective, and measures uncertainty to within 2 mm. Uncertainty propagation was also modeled for the complex mobile manipulator system allowing a generic modeling method to describe, not only the relationships

between systems, but also the mathematical equations in block and parametric diagrams.

The measurement activities and measurement sequence were modeled to provide a step-by-step procedure for performing the mobile manipulator measurement. And lastly, a production use-case was modeled that provides a visual comparison of tasks, actors (those performing the tasks), outcomes, and operation flow for using both measurement methods. More or less detail can be provided in the use-case diagram to instantiate the use-case of the measurement methods to provide the user with information on the best method to implement for their application.

The future of this research is expected to demonstrate an actual production facility utilizing the RMMA mobile manipulator performance measurement method. Actual implementation in industry will most likely uncover further details to add to the models described here, as well as provide performance standards committees additional verification to develop generic performance test methods for mobile manipulators.

Acknowledgments The authors thank Conrad Bock and Mehdi Dadfarnia, Systems Integration Division of the Engineering Laboratory at NIST and Lenny Delligatti of Delligatti Associates for their SysML teachings and guidance.

References

1. Object Management Group Systems Modeling Language (OMG SysML) Tutorial, <http://www.omgsysml.org/INCOSE-OMGSysML-Tutorial-Final-090901.pdf>, September, 2009, accessed December 19 (2016)
2. Palmer, J.R., Crow, M.E., Carson, R.S.: Model-Based Systems Engineering without SysML. Boeing presentation to National Defense Industrial Association Systems Engineering Conference, San Diego, pp. 24–27 (2011)
3. Rahman, M.A.A., Mayama, K., Takasu, T., Yasuda, A., Mizukawa, M.: Model-driven development of intelligent mobile robot using systems modeling language (SysML). In: Mobile Robots - Control Architectures, Bio-Interfacing, Navigation, Multi Robot Motion Planning and Operator Training. Edited by Janusz Bdkowski, ISBN 978-953-307-842-7, 402 pages, Publisher: InTech, Chapters, published (2011)
4. Bostelman, R., Foufou, S., Hong, T.: Modeling performance measurement of mobile manipulators. In: 7th Annual IEEE Int. Conf. on CYBER Technology in Automation, Control, and Intelligent Systems, Waikiki, HA (2017)
5. National Institute of Standards and Technology (NIST) Robotic Systems for Smart Manufacturing Program, <https://www.nist.gov/programs-projects/robotic-systems-smart-manufacturing-program>, accessed February 8 (2017)
6. NDC controller, <http://ndcsolutions.com>, accessed April 5 (2017)
7. Su, H.: Cooperative control of payload transport by mobile manipulator collectives. Master of Science Thesis, Graduate School of the State University of New York Buffalo, New York (2008)
8. Nagatani, K., Yuta, S.: An autonomous mobile manipulator with a functionally distributed control system. In: Proceedings of the International Conference on Automation (ICAUTO-95), India, pp. 12–14 (1995)
9. MasterCal, http://www.americanrobot.com/products_mastercal.html (2005)
10. Atcheson, C.B., Heide, F., Heidrich, W.: CALTag: high precision fiducial markers for camera calibration. Vision, Modeling, and Visualization Conference, Siegen (2010)
11. Dainis, A., Juberts, M.: Accurate remote measurement of robot trajectory motion. Proc. IEEE Int. Conf. Robot. Autom. 2, 92–99 (1985)
12. Mauricio, J., Motta, S.T.: Robot Calibration: Modeling Measurement and Applications, Industrial Robotics: Programming, Simulation and Applications, Huat, L. K. (Ed.), ISBN: 3-86611-286-6, InTech (2006)
13. Lau, K., Hocken, R., Haynes, L.: Robot performance measurements using automatic laser tracking techniques. Robot. Comput. Integr. Manuf. J. 2(3), 227–236 (1985)
14. Conrad, K.L., Shiakolas, P.S., Yih, T.C.: Robotic calibration issues: accuracy, repeatability, and calibration. In: Proceedings of the 8th Mediterranean Conference on Control & Automation (MED 2000), Rio, pp. 17–19 (2000)
15. Gerent, J., Hong, D., Duportal, T., Granger, R.: Inventors; Hexagon Metrology, Inc., assignee. Portable coordinate measurement machine. United States patent US D599,226 (2009)
16. International Organization of Standards, www.iso.org, accessed February 5 (2017)
17. Bostelman, R., Falco, J., Hong, T.: Performance Measurements of Motion Capture Systems used for AGV and Robot Arm Evaluation, Autonomous Industrial Vehicles: From the Laboratory to the Factory Floor, STP1594, Book Chapter 7 (2016)
18. Bostelman, R., Falco, J., Hong, T.: Performance measurements of motion capture systems used for AGV and robot arm evaluation. In: Conference: 6th Computer Vision in Vehicle Technology Workshop (CVVT) at CVPR 2015, Boston (2015)
19. ASTM E3064-16 Standard Test Method for Evaluating the Performance of Optical Tracking Systems that Measure Six Degrees of Freedom (6DOF) Pose, <http://www.astm.org>, accessed February 5 (2017)
20. Bostelman, R., Hong, T., Marvel, J.: Performance measurement of mobile manipulators, p. 2015. SPIE Baltimore, MD (2015)
21. Bostelman, R., Eastman, R., Hong, T., Enein, O.A., Legowik, S., Foufou, S.: Comparison of registration methods for mobile manipulators. In: 19th International Conference on CLAWAR, London (2016)
22. Bostelman, R., Foufou, S., Legowik, S., Hong, T.: p. 2016. Product lifecycle management (PLM), Charleston (2016)
23. Bostelman, R., Hong, T., Messina, E.: Intelligence level performance standards research for autonomous vehicles, FinE-R 2015 The Path to Success: Failures in Real Robots Workshop Intelligent Robot Systems (IROS) 2015, Hamburg, Germany
24. Taylor, B.N., Kuyatt, C.E.: Guidelines for evaluating and expressing the uncertainty of NIST measurement results, 1994 Edition, NIST Technical Note 1297 (1994)
25. Flexline, L.: TS02/06/09. (2008). Leica Geosystems. Accessed 10 February 2017

Roger Bostelman is an Advanced Mobility Systems Engineer at the National Institute of Standards and Technology, Gaithersburg, MD, USA. He was Engineering Project Manager for 25 of his 39 years at NIST, the Intelligent Control of Mobility Systems Program, and many NIST and military technology research and development projects. Roger has designed, built and tested mechanical systems and their interface electronics on robot cranes, robot arms, and autonomous vehicles including the RoboCrane, HLPR (Home Lift, Position, and Rehabilitation) Chair, and several other technologies. He is Chairman of ASTM Committee F45 and serves as experts on ANSI/ITSDF B56.5, ISO 13482, ASTM E57, ASTM F48, and ASTM AC220 standards committees. He holds a B.S. in Electrical Engineering from the George Washington University, an M.S. degree in Technology Management from the University of Maryland University College, and is seeking a PhD in Computer Science at the University of Burgundy, France. He has over 100 publications in books, journals, and conference proceedings and he holds 7 patents.

Sebti Foufou obtained a Ph.D. in computer science in 1997 from the University of Claude Bernard Lyon I, France, for a dissertation on parametric surfaces intersections. He worked with the computer science department at the University of Burgundy, France from 1998 to 2009 as faculty member, then as adjunct professor since Sept. 2009. He also worked in 2005 and 2006, as a temporary guest researcher, at the National Institute of Standards and Technology, Gaithersburg, MD, USA. He is with the Department of Computer Science & Engineering at Qatar University since Sept. 2009. His research interests include geometric modeling and geometric constraint solving for curves and surfaces representations, and image processing for face recognition. He is also interested in data models for product lifecycle management and smart machining systems. He is currently with the Department of Computer Science and Engineering, Qatar University, Doha, Qatar.

Dr. Tsai Hong received her PhD from the University of Maryland at College Park in 1982 and retired from the National Institute of Standards and Technology in 2017 after 35 years of service. She is internationally recognized for her research in perception systems and perception performance evaluation for manufacturing and autonomous vehicle safety applications. She was responsible for algorithm design and software development of several major modules for the ARL perception project; perception for advanced intelligent manufacturing; dynamic 6DOF pose measurement methods for manufacturing applications; the DARPA LAGR program, the Indoor Autonomous Vehicle (IAV) project; the Autonomous road Navigation (AutoNav) project, and the Next Generation Inspection System (NGIS) project. Dr. Hong led the metrology and standards for advanced perception project. In addition, her research activities included real-time vision; world modeling; multi-sensor fusion; temporal fusion for unmanned vehicles and mobile robots; and multi-sensor integration and control for industrial inspection. Dr. Hong served as a doctoral thesis advisor and committee member for various students and has published over 100 articles on the above research areas.

Mili Shah received a PhD in Computational and Applied Mathematics from Rice University. She is currently an Associate Professor of Mathematics at Loyola University Maryland and a Guest Researcher at the National Institute of Standards and Technology. Her research interests include problems in computer vision, robotics, and symmetry detection.